15th International Conference on Fluid Control, Measurements and Visualization
27-30 May, 2019, Naples, Italy

Measurements of liquid surface relief with new 'Moon-Glade' Background Oriented Schlieren technique

Nikolay A. Vinnichenko[1,*], **Alexey V. Pushtaev**[1], **Yulia Yu. Plaksina**[1], **Alexander V. Uvarov**[1]

[1]Faculty of Physics, Lomonosov Moscow State University, Moscow, Russia
[*]corresponding author: nickvinn@yandex.ru

Abstract Measurements of liquid surface topography are performed using new modification of Background Oriented Schlieren technique, which is based on apparent distortion of the background pattern image reflected by the deformed surface. Optical setup comprises a camera and backlit background pattern, both installed above the liquid tank. The camera images the background pattern reflection in the liquid surface. The apparent displacement of background pattern features with respect to the reference image, taken for unperturbed liquid surface, is proportional to the local slope of the surface. This enables one to obtain instantaneous surface relief map by solving Poisson equation. Compared to popular free-surface synthetic Schlieren technique, our approach allows measurements of surface waves over deep liquid layers and topography measurements for opaque liquids or multiphase flows. It is also more sensitive, which enables reliable measurements of perturbations as small as 1 μm. Experiments are performed for propagation of circular surface waves, liquid surface deformation due to heating of horizontal wire installed below the liquid surface and natural convection during evaporation of hot liquid. Attenuation coefficient of gravity-capillary waves is shown to be determined with accuracy about 10% for wave frequencies about 10 Hz. Comparison of the results, obtained in glycerol, distilled water and silicone oil, shows the remarkable difference of surface deformation patterns, observed in liquids, which exhibit Marangoni convection, and liquids, where it is suppressed by the surface film. In distilled water and glycerol elevated surface is always observed in heated regions, whereas in silicone oil the surface relief depends on the competition between the buoyancy-driven and surface-tension-driven flows.
Keywords: free surface, background oriented schlieren, surface waves, convection

1 Introduction

Measuring deformation of liquid free surface in various flows is required in many fields, including studies of surface rheology of clean and contaminated liquid surface [1], interfacial gas transfer [2] and heat transfer in thin liquid films flowing down the heated inclined plates [3]. Also, in low-speed flows surface deformation is related to near-surface pressure field [4], which is hard to measure by other means. Optical measurement techniques have important advantages of being non-intrusive and providing instantaneous maps of surface relief with reasonable spatial resolution.

Recently, free-surface synthetic Schlieren (FS-SS) technique [5], which is based on refractive distortion of the background pattern imaged through deformed interface and cross-correlation image processing, became popular due to its extreme experimental simplicity. It should be noted that essentially the same method had been proposed before by other authors [6][7]. It was employed to measure free surface deformations for meniscus over an inclined flat plate [8], for the waves generated by a droplet bouncing on a vibrating liquid bath [9] and for water striders walking on water surface [10]. Further development involved using the same optical configuration with different background patterns and image processing techniques: dot tracking [11] and 2D Fourier transform profilometry [12]. Also, it was proposed to measure the refraction difference between two wavelengths [13] to measure perturbations with large curvature.

However, FS-SS technique has two important drawbacks. First, since it is based on imaging through the liquid, it is inapplicable for surface topography measurements in opaque liquids, liquids containing optical inhomogeneities or multiphase flows (e.g. boiling liquid films). Second, the distortion is proportional to the distance between the background pattern and liquid surface. This results in severe image blur and cross-correlation interrogation failure for measurements in deep liquid layers. For example, authors of [10] had to keep water depth about 1 mm to measure surface dimples, created by the legs of young water strider instars. A natural way to eliminate these drawbacks is to analyze the reflected image rather than refracted one. The reflective approach for free surface deformation measurements was already implemented using conventional schlieren setup [14]

or color encoding of the incident rays angles similar to rainbow schlieren technique [15][4]. Cross-correlation interrogation has not yet been used. In the present study we perform measurements of free surface deformation using cross-correlation image processing as in FS-SS technique or in Background Oriented Schlieren (BOS) [16], but with reflective optical scheme. Besides the assessment of new experimental technique, we focus on dissimilarity of surface deformation patterns observed in liquids with different surface behavior: silicone oil, which exhibits Marangoni convection, and glycerol and distilled water, where it is known to be suppressed by the presence of surface film [17][18]. The proposed technique, able to measure surface perturbations as small as 1 μm, allows clear demonstration of the effect of Marangoni flow on free surface deformation. The rest of the paper is organized as follows. In Section 2 the employed experimental technique is described and compared to FS-SS and fringe projection profilometry. Experimental results for three flows under study: (1) circular surface waves, (2) convective plume, produced by a horizontal heated wire and impacting the free surface, (3) natural convection during evaporation of hot liquid – are presented and discussed in Section 3. Finally, the conclusions are summarized in Section 4.

2 Experimental technique

The optics of the proposed technique is shown in Fig. 1a. The background pattern, printed on a transparent film and backlit with LED panel, is installed above the liquid tank at an angle to horizontal, so that the camera, which is also inclined, images the background pattern reflection.

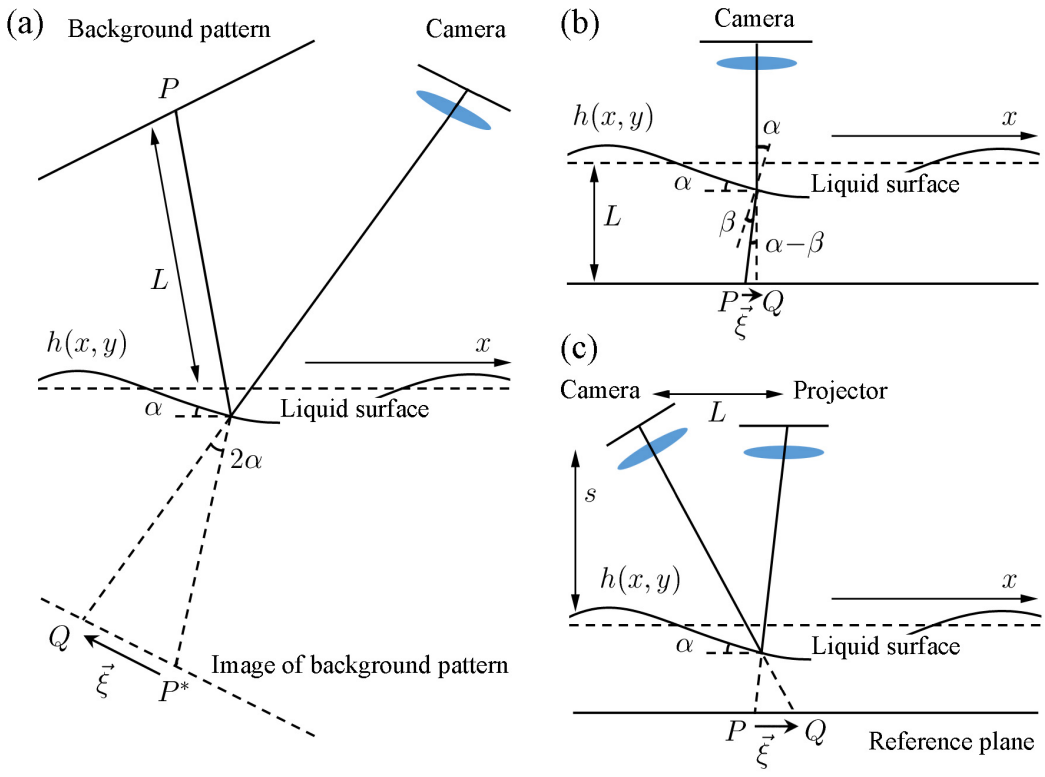

Fig. 1 Optical configurations of three surface deformation measurement techniques. (a) The proposed Moon-Glade Background Oriented Schlieren, (b) FS-SS technique [5], (c) fringe projection profilometry [19][20].

As in FS-SS technique, reference image is taken for undisturbed surface, which is then digitally compared to images obtained in presence of perturbations. Free surface deformation results in deflection of reflected rays and distortion of the background pattern image – similarly to moon-glade due to water ripples at sea. For small surface slopes the light rays, reflected from the deformed surface, are deflected from the original path by the angle equal to twice the local slope of the surface. Hence, in paraxial approximation the apparent displacement

of background pattern features is

$$\xi_x = 2L\frac{\partial h}{\partial x}, \tag{1}$$

where L is the distance between the background pattern and liquid surface. Similarly,

$$\xi_y = 2L\frac{\partial h}{\partial y}, \tag{2}$$

which enables one to obtain instantaneous surface relief map $h(x,y)$ either by solving Poisson equation

$$\frac{\partial^2 h}{\partial x^2} + \frac{\partial^2 h}{\partial y^2} = \frac{a_{back}}{2La_{surf}}\left(\frac{\partial \xi_x}{\partial x} + \frac{\partial \xi_y}{\partial y}\right)_{pix} \tag{3}$$

with appropriate boundary conditions or using least-squares solution of overdetermined system of first-order equations (1)-(2). Note that derivatives in the left-hand side of Eq. (3) are taken with respect to coordinates along the liquid surface, whereas in the right-hand side both the displacement components and coordinates are measured in pixels. a_{back} and a_{surf} stand for image resolution (m/pix) in the background pattern plane and liquid surface plane, respectively. Since the camera images liquid surface obliquely, raw images are to be corrected for keystone distortion. This is performed using calibration image of rectangular target, the corners of which determine coefficients of projective transform. However, bright light source allows operation in moderate incidence angle range 5–20 ° (water surface reflectance is about 0.02), where the keystone effect is not strong.

In FS-SS technique, presented in Fig. 1b, the background pattern is installed below the liquid layer and the camera images it through the interface. In this case the apparent displacement due to refraction is

$$\xi_x = -L\frac{n-1}{n}\frac{\partial h}{\partial x}, \tag{4}$$

where n is the liquid refractive index. As mentioned above, FS-SS technique is only applicable to transparent liquids without significant optical inhomogeneities. Comparison of Eqs. (1) and (4) shows that Moon-Glade BOS is more sensitive with respect to FS-SS technique (8 times more sensitive for water). This enables one to measure surface perturbations as small as 1 μm. However, large sensitivity results also in large displacement gradient for surface waves with large curvature. Strong image blur can also be observed, because different rays from the same point of background pattern are reflected (or refracted) by the surface regions with different slopes and experience different deflections.

$$\frac{\partial \xi_x}{\partial x} = KL\frac{a_{surf}}{a_{back}}\frac{\partial^2 h}{\partial x^2}, \tag{5}$$

where

$$K = \begin{cases} 2, & \text{Moon-Glade BOS} \\ -\frac{n-1}{n}, & \text{FS-SS} \end{cases} \tag{6}$$

This effect, described by invertibility condition in [5], is also well-known in BOS [21]. Multi-pass cross-correlation interrogation provides reliable displacement values for displacement gradients up to 0.4–0.5 pix/pix. Thus, if the liquid under study is transparent, choice between Moon-Glade BOS and FS-SS technique depends on perturbations magnitude and surface curvature in specific application.

Another optical technique, which is often used to measure surface shape, is fringe projection profilometry (FPP) (Fig. 1c). Like Moon-Glade BOS, it is based on analysis of the reflected image and is applicable for measurements in opaque liquids. The difference is that diffuse reflection is employed in FPP, whereas Moon-Glade BOS makes use of specular reflection. As a result, the apparent displacement in FPP is determined by the local elevation of liquid surface with respect to the reference plane rather than the liquid surface slope. In FPP

$$\xi_x = \frac{L}{s/h-1} \approx \frac{Lh}{s} \tag{7}$$

for the camera and projector located at the same height s and separated by the distance L. Since L and s are of the same order of magnitude, FPP is much less sensitive in comparison with Moon-Glade BOS and FS-SS and is typically used to measure liquid surface perturbations about 1 mm. Another consequence of using diffuse reflection in FPP is that small amount of white dye had to be added to water both in [19] and [20] to enhance light diffusivity of the liquid surface. It was supposed that the dye does not affect surface properties. In contrast, Moon-Glade BOS does not require dye addition, since it is based on specular reflection.

3 Results and discussion

3.1 Circular surface waves

Measurements of instantaneous free surface relief maps for gravity-capillary waves enable one to compare wave profiles obtained in experiment with theory and to determine the complex wavenumber $k = k_0 + i\gamma$, which is related to radian frequency ω by dispersion relation [22]

$$\left(2 - i\frac{\omega}{\nu k^2}\right)^2 + \frac{g}{\nu^2 k^3} + \frac{\sigma}{\nu^2 k \rho} = 4\sqrt{1 - i\frac{\omega}{\nu k^2}} \tag{8}$$

ν, ρ and σ are, respectively, kinematic viscosity, density and surface tension of the liquid. Attenuation coefficient γ is affected by surface rheology, so it can be used to measure surface tension or viscosity, or to study elasticity of liquid surface contaminated with surfactants [1]. Using point source to excite circular waves has the advantage of reducing edge effects, which lead to formation of transverse waves and are unavoidable in plane configuration.

The experiments are performed in a cylindrical tank with diameter 25 cm filled with silicone oil PDMS-10 (kinematic viscosity 10 cSt, density 935 kg/m^3, surface tension 20.1 mN/m). Liquid layer depth is 21 mm. The waves were generated using a plastic cylinder 5-mm in diameter, connected to a speaker. Images of backlit background pattern, composed of transparent square dots randomly distributed over a black area (dot image size about 3 pix), are obtained at 50 fps with Canon EOS 700D camera equipped with Canon EF 100 mm f/2.8 lens. Incidence angle is 19.6°, background-to-surface and lens-to-surface distances are 32 and 173 cm, respectively. Cross-correlation processing involves three interrogation passes with interrogation window size decreasing from 32×32 to 16×16 and overlap 50% at the final pass. Fig. 2 presents the results obtained for the frequency 8 Hz. The wave profile is described by

$$h(r,t) = h_0 e^{-i\omega t} H_0^{(1)}(kr), \tag{9}$$

where $H_0^{(1)}$ is Hankel function of the first kind. Eq. (9) can be used to fit experimental surface elevation data. However, when the waves cover the whole measurement region, Dirichlet boundary condition for Poisson equation (3), which is imposed at the right boundary, becomes invalid. Hence, it is preferable to fit the original absolute displacement data rather than surface elevation field. Absolute displacement fit

$$|\vec{\xi}(x,y,t)| = \left| \Re\left\{ \xi_0 k e^{-i\varphi} H_1^{(1)}\left(k\sqrt{(x-x_0)^2 + (y-y_0)^2} \right) \right\} \right| \tag{10}$$

contains six unknown parameters (recall that k is complex). They are determined using nonlinear least-squares regression for each instantaneous absolute displacement field. Since large displacement gradients are observed near the wave generator and at large distances the wave amplitude becomes comparable with the noise of cross-correlation interrogation, only the data for radial positions $3 \le r \le 10$ are taken into account. Fig. 2d presents the fitted wave profile and experimental points for one of the frames. Despite the relatively low camera frame rate, the temporal behavior of the wrapped phase φ, shown in Fig. 2e, is in good agreement with theoretical dependence, which confirms high quality of the fit. The experimentally determined complex wavenumber is $k_{exp} = [(231.8 \pm 1.7) + (8.4 \pm 0.8)i]$ m^{-1}. Standard deviations of fit parameters for the series of 170 images are given as uncertainty estimates. This matches well theoretical prediction $k_{theory} = [230.9 + 8.1i]$ m^{-1}. Note that attenuation coefficient uncertainty about 10% is slightly less than estimated in [1] for pointwise measurement of circular wave field based on refraction of a laser beam. Much better accuracy (0.1% for attenuation coefficient) was reported in [23] for interferometric measurements of extremely weak waves (~ 0.1 μm), but only at frequencies exceeding 1 kHz, for which parasitic surface oscillations can be efficiently filtered out.

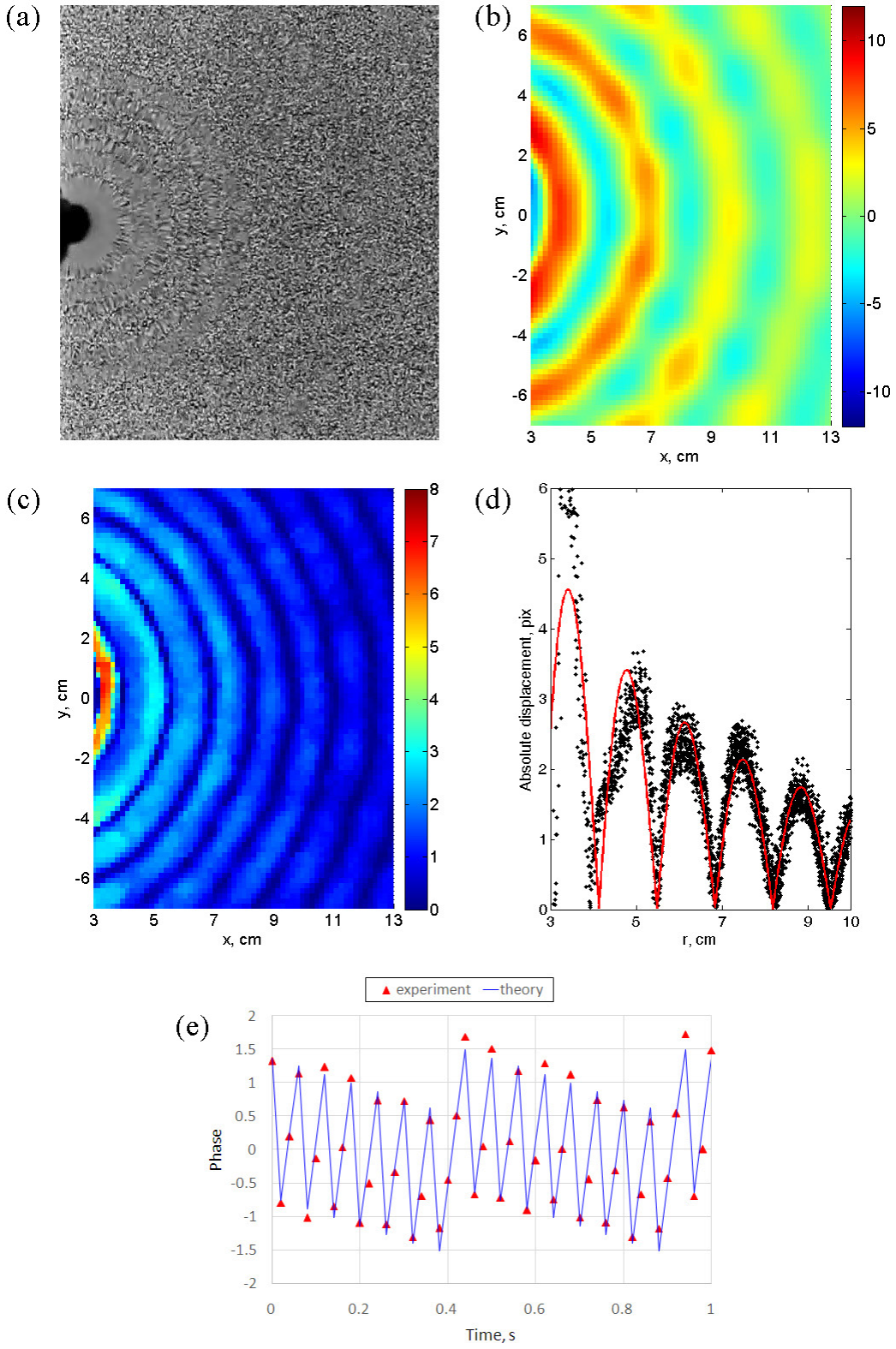

Fig. 2 Measurements of circular surface waves in PDMS-10. (a) Original image, (b) surface elevation field (μm), (c) absolute displacement field (pix), (d) wave profile fit, (e) temporal dependence of phase φ.

3.2 Convective plume impacting the free surface

Free surface deformation due to natural convection in heated liquids results from opposing effects of buoyancy forces and Marangoni convection. Marangoni convection leads to formation of concave troughs over the heated

regions, because liquid is transported by surface-tension-induced flow from hot regions of the surface to cold ones. In contrast, buoyancy produces convex crests in hot regions due to rising currents impacting the free surface. The relative importance of these two effects depends on liquid layer depth and surface properties of the liquid. A convenient experimental configuration to study surface deformation and heat transfer in the surface layer, associated with natural convection, is the convective plume from a horizontal heated wire, installed below the liquid surface. It was studied in [17] using BOS, infrared thermography and numerical simulations. However, free surface deformation was only obtained numerically for two different boundary conditions, representing the surface behavior of distilled water and ethanol. Surface relief was measured in [14] using reflective modification of conventional schlieren setup. Both concave and convex surface profiles were obtained in silicone oil and aqueous glycerol solution for different pool depths. However, it was implicitly assumed that surface shape is steady. As shown below, this is not the case, especially in liquids, which exhibit Marangoni convection.

Moon-Glade BOS experiments are performed for glycerol and silicone oil PDMS-5 (kinematic viscosity 5 cSt, density 918 kg/m^3, surface tension 19.7 mN/m, surface tension temperature coefficient $-6.6 \cdot 10^{-5}$ Nm^{-1}K^{-1}) in a rectangular tank $123 \times 131 \times 66$ mm. Copel wire is installed horizontally at depth 7 and 5 mm below the liquid surface for experiments in glycerol and silicone oil, respectively. Liquid layer depth is 30 mm, heating power is 18.4 W/m. Values of the optical setup parameters are presented in Table 1. As in Section 3.1, two interrogation passes are performed with interrogation window size decreasing from 32×32 to 16×16 and overlap 50% at the final pass.

Table 1 Moon-Glade BOS setup parameters for convective plume experiments

liquid	incidence angle, $^\circ$	background-to-surface distance, cm	lens-to-surface distance, cm	frame rate, fps
glycerol	20	19.5	46	1
PDMS-5	14.4	28	185	50

Results of experimental measurements are compared to numerical simulations, performed with the same code as in [17] (second-order semi-implicit scheme for 2D Navier-Stokes equations in low-Mach approximation). Silicone oil is known to exhibit Marangoni convection, whereas in glycerol it is suppressed by the presence of surface film. Thus, as ethanol and distilled water in [17] and [18], these two liquids can be used as representatives of two different kinds of surface behavior, which correspond to different boundary conditions for horizontal velocity at free surface in 2D numerical simulations. No-slip condition $V_x = 0$ is specified for glycerol and tangential-stress condition

$$\frac{\partial V_x}{\partial z} = \frac{1}{\eta}\frac{\partial \sigma}{\partial x} - \frac{\partial V_z}{\partial x}, \tag{11}$$

which takes into account Marangoni effect, is used for simulations in silicone oil (z-axis is directed upwards). As in [17], surface deformation is described by

$$p_{air} - p + \rho g h - \sigma \frac{\partial^2 h}{\partial x^2} + 2\eta \frac{\partial v_z}{\partial z} = 0 \tag{12}$$

Computational grid 100×110 is used with the grid step varying from 0.06 mm near the surface and close to the heated wire to 11 mm near the bottom of the tank.

Fig. 3 presents experimental and numerical results for horizontal heated wire in glycerol. Since Marangoni convection is suppressed by the surface film, glycerol surface behavior is well described by no-slip condition, which is confirmed by good agreement between Moon-Glade BOS data and simulations. Note that Moon-Glade BOS, being sensitive to surface slope, does not take into account the total change of the liquid level. For ease of comparison, boundary condition $h = 0$ is used both at the far-from-the-wire boundaries in Moon-Glade BOS and at the tank walls in numerical simulations. Convective plume impact results in formation of a single crest above the heated wire, which grows as long as heating continues. In contrast, the results for silicone oil, shown in Fig. 4, demonstrate the formation of a traveling wave, which contains central peak, surrounded by

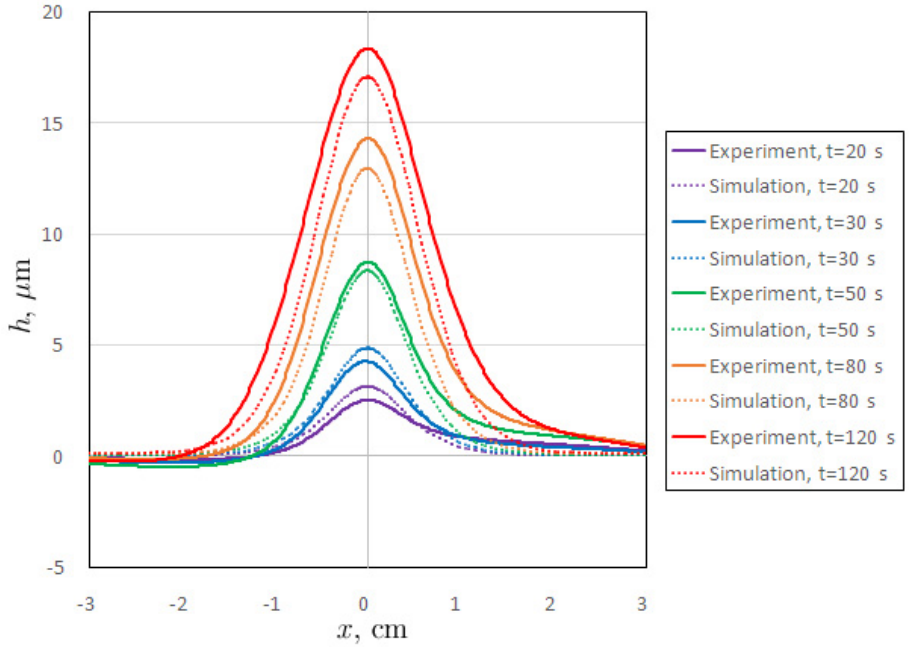

Fig. 3 Surface profiles for horizontal heated wire in glycerol at different time instants after heating is initiated.

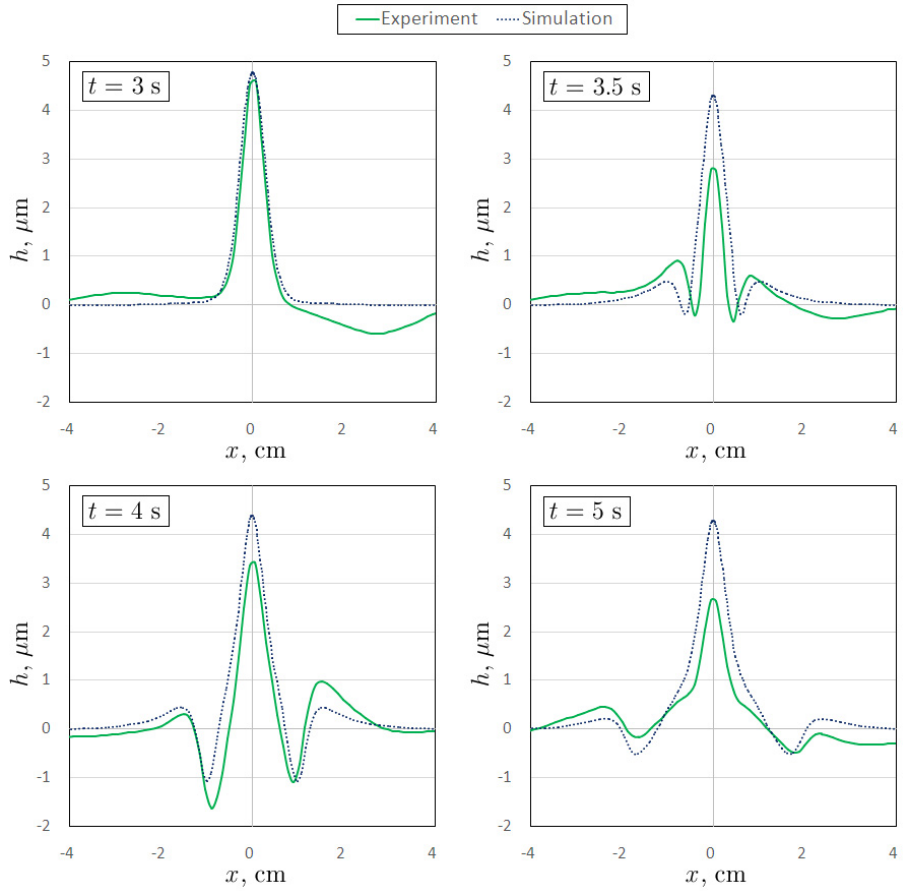

Fig. 4 Surface profiles for horizontal heated wire in PDMS-5 at different time instants after heating is initiated.

two concave troughs. These troughs propagate away from the wire and finally reflect from the tank walls (not shown). Although there are some discrepancies between experimental and numerical values of the central peak height, the shape of the surface wave and the location of troughs at different time instants are quite similar. This

confirms both the accuracy of Moon-Glade BOS measurements and the validity of using boundary condition Eq. (11) to describe surface behavior of liquids, which exhibit Marangoni convection.

3.3 Natural convection in evaporating liquid heated from below

Free surface deformation is also measured for Rayleigh-Bénard convection in liquids heated from below. Experimental setup configuration is shown in Fig. 5. To investigate the relation between the surface shape and temperature, we perform simultaneous measurements of surface deformation using Moon-Glade BOS and surface temperature using infrared thermography. FLIR SC7700-M infrared camera is used, operating in wavelength range 3.7–4.8 μm. Distilled water and silicone oil PDMS-10 are used to compare the results in liquids with different surface behavior. Experiments are performed in an open latten cuvette $140 \times 130 \times 18$ mm. Liquid layer depth is 8 and 6 mm for experiments in distilled water and silicone oil, respectively. The incidence angle for Moon-Glade BOS is 6°, background-to-surface and lens-to-surface distances are 77 and 98 cm, respectively. Four interrogation passes with interrogation window size decreasing from 32×32 to 8×8 are performed to obtain the apparent displacement field in water. In PDMS-10 larger displacement gradients are observed. Therefore, interrogation involves three passes with window size decreasing from 20×20 to 10×10. Overlapping interrogation windows are employed at the final pass in both cases, so that the displacement field is obtained for a grid with 4 pixels pitch.

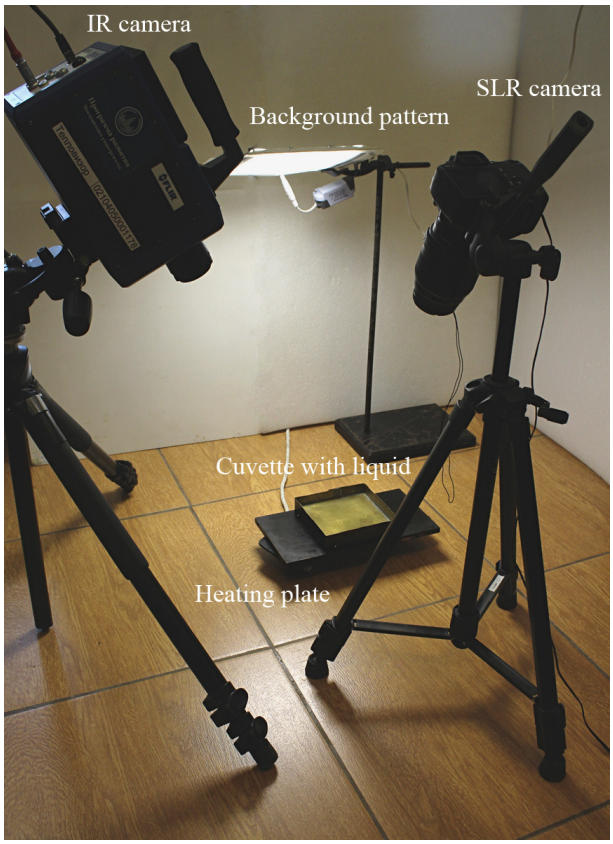

Fig. 5 Experimental setup for simultaneous measurements of surface deformation and surface temperature fields.

Fig. 6 presents surface elevation and surface temperature distributions in the common field of view, shared by IR and SLR cameras. Despite Moon-Glade BOS has lower spatial resolution in comparison with surface temperature measurement using IR camera, it is obvious from Figs. 6a and 6b that in water surface crests and troughs correspond, respectively, to warm and cold surface regions. This is also observed at higher temperatures, up to 60°C. In contrast, in PDMS-10 surface elevation and surface temperature fields are similar only at low temperatures. The results for the average surface temperature about 40°C, shown in Figs. 6c and 6d, demonstrate some discrepancy. On the one hand, the locations of surface peaks coincide with warm centers of polygonal Bénard cells, observed in surface temperature data. On the other hand, the crest and trough near

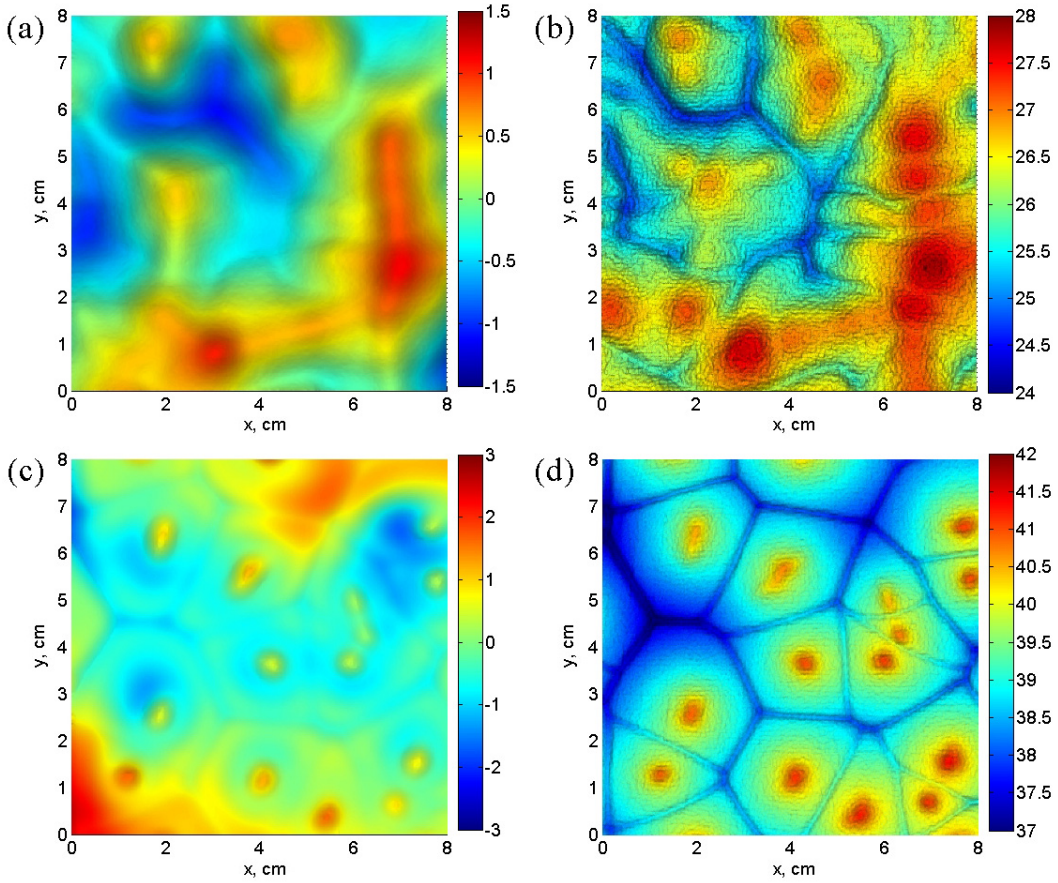

Fig. 6 Surface elevation fields (left column, μm) and surface temperature fields (right column, °C) for natural convection in distilled water (upper row) and PDMS-10 (lower row) heated from below.

the top-right corner correspond to regions of low and high surface temperature. This indicates the effect of Marangoni convection on surface deformation. It is expected that with less deep layers of silicone oil the complete transition can be obtained from similarity of surface elevation and temperature perturbations to them being opposite in sign.

4 Conclusions

In this study, subtle deformations of liquid surface have been measured using new modification of Background Oriented Schlieren technique (Moon-Glade BOS), which is based on cross-correlation analysis of the background pattern image reflected by the deformed surface. It is more sensitive in comparison with popular FS-SS technique and allows measurements of surface relief for deep liquid layers, opaque liquids and flows, which contain optical inhomogeneities, including multiphase flows. Unlike fringe projection profilometry, it makes use of specular reflection rather than diffuse one, so it does not require addition of dye, which can alter surface properties. As for FS-SS technique, the major limitations are image blur and large displacement gradients, which are observed for surface perturbations with large curvature.

Measurements have been performed for the circular gravity-capillary waves, free surface deformation due to impact of convective plume from a horizontal heated wire and Rayleigh-Bénard convection in liquid heated from below. It is demonstrated that Moon-Glade BOS enables one to measure attenuation coefficient of the surface waves with accuracy about 10% for wave frequencies about 10 Hz. This can be used to study rheology of liquid surface, contaminated with surfactants, using simple and cheap experimental equipment. For natural convection flows surface deformations in liquids with different surface behavior are compared. It is shown that in glycerol, where Marangoni convection is suppressed by the surface film, a single crest is formed above the heated wire. In contrast, in silicone oil unsteady wave is observed, composed of stagnant central

peak, surrounded by two moving troughs. For both liquids surface deformation is well described by numerical simulations with appropriate boundary condition for horizontal velocity at the liquid surface: no-slip condition for glycerol and tangential-stress condition, which takes into account Marangoni effect, for silicone oil. Simultaneous measurements of surface relief and surface temperature for Rayleigh-Bénard convection also show different behavior in different liquids. In distilled water the fields of surface elevation and surface temperature are similar: crests and troughs correspond, respectively, to warm and cold surface regions. In silicone oil influence of Marangoni convection upon the surface relief is observed, which is opposite to buoyancy effect. Thus, in liquid, which exhibits Marangoni convection, the relation between the surface deformation and surface temperature is determined by the relative importance of these two effects, which depends on liquid layer depth.

Acknowledgments

Authors acknowledge the support from M.V. Lomonosov State University Program of Development.

References

[1] Saylor J R, Szeri A J, Foulks G P (2000) Measurement of surface properties using a circular capillary wave field. *Experiments in Fluids*, vol. 29, pp 509-518. doi: 10.1007/s003480000119

[2] Turney D E, Banerjee S (2013) Air-water gas transfer and near-surface motions. *Journal of Fluid Mechanics*, vol. 733, pp 588-624. doi: 10.1017/jfm.2013.435

[3] Markides C N, Mathie R, Charogiannis A (2016) An experimental study of spatiotemporally resolved heat transfer in thin liquid-film flows falling over an inclined heated foil. *International Journal of Heat and Mass Transfer*, vol. 93, pp 872-888. doi: 10.1016/j.ijheatmasstransfer.2015.10.062

[4] Dabiri D, Gharib M (2001) Simultaneous free-surface deformation and near-surface velocity measurements. *Experiments in Fluids*, vol. 30, pp 381-390. doi: 10.1007/s003480000212

[5] Moisy F, Rabaud M, Salsac K (2009) A synthetic Schlieren method for the measurement of the topography of a liquid interface. *Experiments in Fluids*, vol. 46, pp 1021-1036. doi: 10.1007/s00348-008-0608-z

[6] Murase H (1992) Surface shape reconstruction of a nonrigid transparent object using refraction and motion. *IEEE Transactions on Pattern Analysis and Machine Intelligence*, vol. 14, pp 1045-1052. doi: 10.1109/34.159906

[7] Fouras A, Hourigan K, Kawahashi M, Hirahara H (2006) An improved, free surface, topographic technique. *Journal of Visualization*, vol. 9, pp 49-56. doi: 10.1007/BF03181568

[8] Mishra A, Kulkarni V, Khor J-W, Wereley S (2015) Mapping surface tension induced menisci with application to tensiometry and refractometry. *Soft Matter*, vol. 11, pp 5619-5623. doi: 10.1039/C5SM00497G

[9] Damiano A P, Brun P-T, Harris D M, Galeano-Rios C A, Bush J W M (2016) Surface topography measurements of the bouncing droplet experiment. *Experiments in Fluids*, vol. 57, 163. doi: 10.1007/s00348-016-2251-4

[10] Steinmann T, Arutkin M, Cochard P, Raphaël E, Casas J, Benzaquen M (2018) Unsteady wave pattern generation by water striders. *Journal of Fluid Mechanics*, vol. 848, pp 370-387. doi: 10.1017/jfm.2018.365

[11] Charruault F, Greidanus A J, Breugem W-P, Westerweel J (2018) A dot tracking algorithm to measure free surface deformations. In: Proceeding of the 18th International Symposium on Flow Visualization, pp 318-319.

[12] Wildeman S (2018) Real-time quantitative Schlieren imaging by fast Fourier demodulation of a checkered backdrop. *Experiments in Fluids*, vol. 59, 97. doi: 10.1007/s00348-018-2553-9

[13] Kolaas J, Riise B H, Sveen K, Jensen A (2018) Bichromatic synthetic schlieren applied to surface wave measurements. *Experiments in Fluids*, vol. 59, 128. doi: 10.1007/s00348-018-2580-6

[14] Kayser W V, Berg J C (1973) Surface relief accompanying natural convection in liquid pools heated from below. *Journal of Fluid Mechanics*, vol. 57, pp 739-752. doi: 10.1017/S0022112073001989

[15] Zhang X, Dabiri D, Gharib M (1996) Optical mapping of fluid density interfaces: Concepts and implementations. *Review of Scientific Instruments*, vol. 67, pp 1858-1868. doi: 10.1063/1.1146990

[16] Meier G E A (2002) Computerized Background-Oriented Schlieren. *Experiments in Fluids*, vol. 33, pp 181-187. doi: 10.1007/s00348-002-0450-7

[17] Vinnichenko N A, Uvarov A V, Plaksina Yu Yu (2014) Combined study of heat exchange near the liquid–gas interface by means of Background Oriented Schlieren and Infrared Thermal Imaging. *Experimental Thermal and Fluid Science*, vol. 59, pp 238-245. doi: 10.1016/j.expthermflusci.2013.11.023

[18] Vinnichenko N A, Pushtaev A V, Plaksina Yu Yu, Rudenko Yu K, Uvarov A V (2018) Horizontal convection driven by nonuniform radiative heating in liquids with different surface behavior. *International Journal of Heat and Mass Transfer*, vol. 126, pp 400-410. doi: 10.1016/j.ijheatmasstransfer.2018.06.036

[19] Cobelli P J, Maurel A, Pagneux V, Petitjeans P (2009) Global measurement of water waves by Fourier transform profilometry. *Experiments in Fluids*, vol. 46, pp 1037-1047. doi: 10.1007/s00348-009-0611-z

[20] Zhang K, Wei T, Hu H (2015) An experimental investigation on the surface water transport process over an airfoil by using a digital image projection technique. *Experiments in Fluids*, vol. 56, 173. doi: 10.1007/s00348-015-2046-z

[21] Gojani A B, Kamishi B, Obayashi S (2013) Measurement sensitivity and resolution for background oriented schlieren during image recording. *Journal of Visualization*, vol. 16, pp 201-207. doi: 10.1007/s12650-013-0170-5

[22] Lamb H (1916) Hydrodynamics, 4th ed. Cambridge University Press, Cambridge.

[23] Shmyrov A, Mizev A, Shmyrova A, Mizeva I (2019) Capillary wave method: An alternative approach to wave excitation and to wave profile reconstruction. *Physics of Fluids*, vol. 31, 012101. doi: 10.1063/1.5060666